

Report

IQGAP-Related Rng2p Organizes Cortical Nodes and Ensures Position of Cell Division in Fission Yeast

Anup Padmanabhan,^{1,2,4} Kavya Bakka,^{1,2,4} Mayalagu Sevugan,¹ Naweed I. Naqvi,^{1,2} Ventris D'souza,¹ Xie Tang,¹ Mithilesh Mishra,^{1,*} and Mohan K. Balasubramanian^{1,2,3,*}

¹Temasek Life Sciences Laboratory

²Department of Biological Sciences

³Mechanobiology Institute

The National University of Singapore, 1 Research Link, Singapore 117604, Singapore

Summary

Correct positioning of the cell division machinery is crucial for genomic stability and cell fate determination. The fission yeast *Schizosaccharomyces pombe*, like animal cells, divides using an actomyosin ring and is an attractive model to study eukaryotic cytokinesis. In *S. pombe*, positioning of the actomyosin ring depends on the anillin-related protein Mid1p [1–3]. Mid1p arrives first at the medial cortex and recruits actomyosin ring components to node-like structures [4–7], although how this is achieved is unknown. Here we show that the IQGAP-related protein Rng2p, an essential component of the actomyosin ring [8, 9], is a key element downstream of Mid1p. Rng2p physically interacts with Mid1p and is required for the organization of other actomyosin ring components into cortical nodes. Failure of localization of Rng2p to the nodes prevents medial retention of Mid1p and leads to actomyosin ring assembly in a node-independent manner at nonmedial locations. We conclude that Mid1p recruits Rng2p to cortical nodes at the division site and that Rng2p, in turn, recruits other components of the actomyosin ring to cortical nodes, thereby ensuring correct placement of the division site.

Results and Discussion

IQGAP-family proteins, such as Rng2p, contain multiple domains, including a calponin-homology domain, IQ sequence motifs, a RAS-GAP related domain (GRD), and a RAS-GAP C-terminal homology domain (RasGAP-C) (Figure 1A) [8–12]. Because a protein such as Rng2p, with multiple domains, might regulate cytokinesis through multiple mechanisms, we carried out a random mutagenesis of *rng2* to isolate new alleles with potentially different phenotypes [13]. We isolated a new recessive and nonlethal temperature-sensitive mutant, *rng2-M1*, which is defective in actomyosin ring positioning but not in its assembly. Nucleotide sequencing of the *rng2-M1* locus revealed the potential for three amino acid substitutions in Rng2-M1p, which mapped to the GRD and the RasGAP-C domains (Figure 1A).

To better characterize the *rng2-M1* phenotype, we stained wild-type and *rng2-M1* cells grown at 24°C and shifted them to 30°C or 36°C with DAPI and aniline blue to visualize nuclei

and septa, respectively. *mid1-18*, which is defective in ring positioning [1, 14, 15], and *rng2-D5*, which is defective in actomyosin ring organization [8], served as additional controls. All wild-type cells and the majority of *mid1-18* and *rng2-D5* cells contained medial septa at 24°C and 30°C (Figure 1B). However, division septa in 25% of *rng2-M1* cells were misplaced at 24°C and 30°C (Figure 1B). At 36°C, the percentage of misplaced septa increased in *mid1-18* and *rng2-M1* cells (Figures 1B and 1C). Although *rng2-D5* contained abnormal septa, only a small fraction of these were misplaced (Figures 1B and 1C). These observations established that *rng2-M1* was primarily defective in division septum placement. Because the division septum is assembled at the position of the actomyosin ring, we stained wild-type, *rng2-M1*, and *mid1-18* grown at 30°C to visualize F-actin. Actomyosin rings were indeed misplaced in binucleate *rng2-M1* and *mid1-18* cells (Figures 1D and 1E).

Actomyosin rings are assembled early in mitosis in wild-type cells. By contrast, actomyosin rings are assembled later in mitosis in *mid1-18* cells [2, 4]. To assess the stage of mitosis in which rings assemble in *rng2-M1*, we stained wild-type and *rng2-M1* with antibodies against Cdc4p (EF hand protein that binds to Rng2p and Myo2p [16, 17]) and tubulin (Figures 1F and 1G). Early mitotic wild-type cells (spindle length < 4 μm) displayed Cdc4p in the form of cortical-medial nodes (cell 1 in Figure 1F) or in medial rings, neither of which were detected in *rng2-M1* cells (cell 1a in Figure 1F). Neither rings nor cortical nodes of Cdc4p were detected in *rng2-M1* cells with intermediate-length spindles of 4–8 μm (compare cells 2 and 2a in Figure 1F). Misplaced rings were detected in a majority of *rng2-M1* cells with fully elongated spindles (compare cells 3 and 3a in Figure 1F). In essentially all wild-type and *rng2-M1* cells with a postanaphase array of microtubules, actomyosin rings were detected (cell 4a in Figure 1F; data not shown for wild-type). These observations established that ring assembly occurred later in mitosis in *rng2-M1* mutants. Genetic analysis (see Figure S1 available online) established that Rng2p and Mid1p function in the same pathway to position the ring. Assembly of the misplaced rings in *rng2-M1* required the septation initiation network, a signaling cascade essential for ring assembly, maturation, and stability in late mitosis [7, 18–21] (data not shown).

To understand the mechanism of ring misplacement in *rng2-M1*, we investigated the localization of GFP-tagged Rng2-M1p. In wild-type cells with short spindles, Rng2p-GFP localized to a series of medial nodes or rings (Figures 2A and 2B). In *rng2-M1* mutants with short spindles, however, Rng2-M1p-GFP did not localize to cortical nodes or rings (Figures 2A and 2B), although it was detected in actomyosin rings during late mitosis (Figure S2A). The analysis of Rng2-M1p localization, taken together with our work (Figure S2B) and the work of others [9], established that the C terminus of Rng2p, and not the calponin homology domain (CHD) or IQ motifs, targeted it to the cortical nodes.

Because Rng2-M1p and Cdc4p failed to localize to cortical nodes in *rng2-M1*, we assessed whether other actomyosin ring components were similarly affected. Mid1p assembled at the nucleus and cortical nodes in 50 out of 50 uninucleate

*Correspondence: mishra@tli.org.sg (M.M.), mohan@tli.org.sg (M.K.B.)

⁴These authors contributed equally to this work

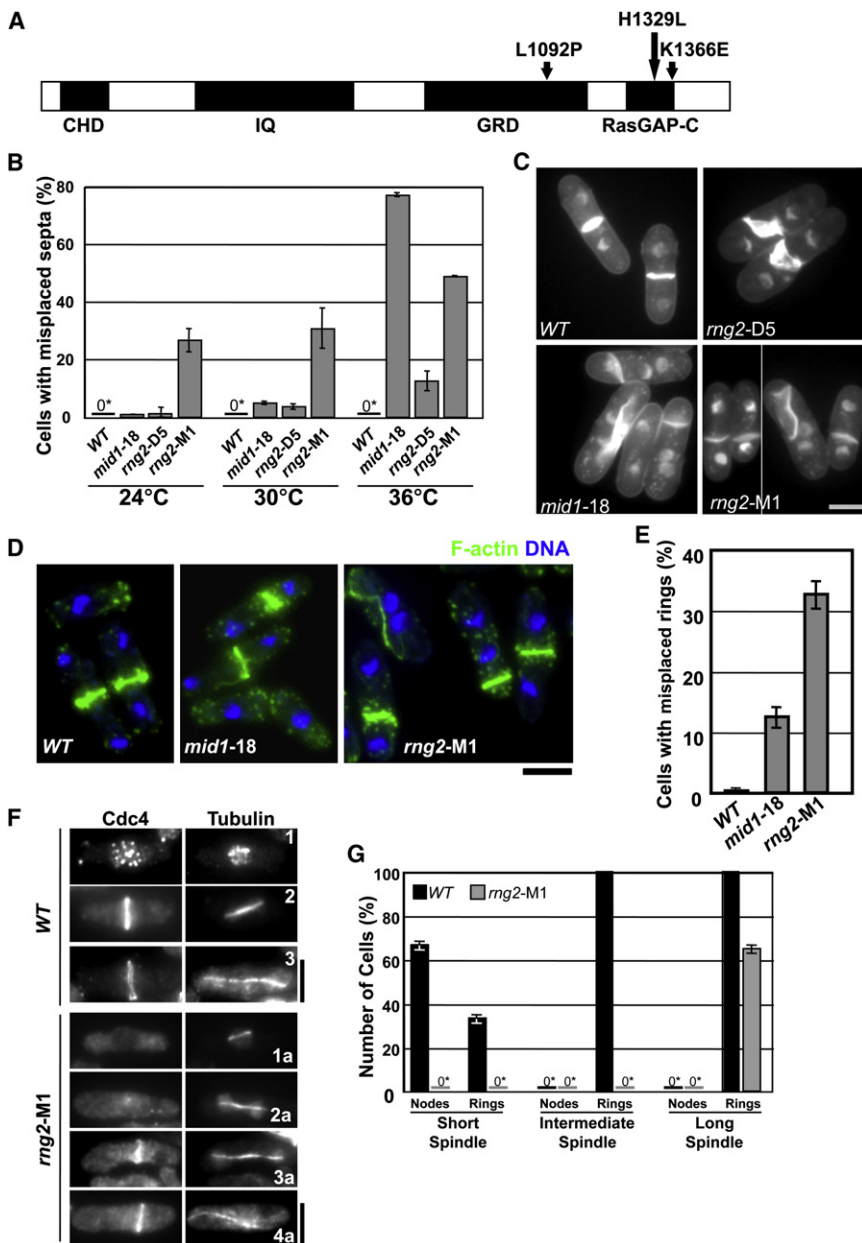


Figure 1. *rng2*-M1 Mutants Are Defective in Positioning the Actomyosin Ring and Division Septa and Assemble Rings Late in Mitosis

(A) Domain map of Rng2p highlighting the amino acid changes in the *rng2*-M1 allele. The amino acid changes fall in the GAP-related domain (GRD) and the Ras-GAP-C-terminal homology domain (RasGAP-C).

(B) Division septa are misplaced in *rng2*-M1 cells. Wild-type (WT), *rng2*-D5, *mid1*-18, and *rng2*-M1 cells were harvested following 4 hr shift from 24°C to 30°C and 36°C and were fixed and stained with DAPI and aniline blue; the proportion of cells with misplaced septa was quantitated. Mean ± standard deviation (SD; error bars) was calculated based on three independent experiments (n = 500).

(C) Images of cells of the indicated genotypes incubated at 36°C and stained with aniline blue and DAPI to visualize septa and nuclei, respectively.

(D) Actomyosin rings are misplaced in *rng2*-M1. WT, *mid1*-18, and *rng2*-M1 cells grown at 24°C and shifted to 30°C for 4 hr were fixed, permeabilized, and stained with AlexaFluor 488-phalloidin and DAPI.

(E) Quantification of the phenotypes described in (D). Mean ± SD (error bars) was calculated based on three independent experiments (n = 500).

(F) *rng2*-M1 cells assemble rings late in mitosis. WT and *rng2*-M1 cells were grown at 24°C, shifted to 30°C, fixed, and stained with Cdc4p and tubulin antibodies. WT (panels 1, 2, and 3) and *rng2*-M1 (panels 1a, 2a, 3a, and 4a) shown represent cells with short (<4 μm; cells 1 and 1a), intermediate (4 μm to 8 μm; cells 2 and 2a), and long (>8 μm; cells 3 and 3a) spindles. Panel 4a represents a *rng2*-M1 cell with a postanaphase array of microtubules and a misplaced actomyosin ring. (G) Quantification of WT and *rng2*-M1 cells with short, intermediate, and long spindle containing cdc4p in cortical nodes or fully formed actomyosin rings. Mean ± SD (error bars) was calculated based on three independent counts (n = 50 for each stage). Scale bar represents 5 μm. See also Figure S1.

wild-type and 50 out of 50 uninucleate *rng2*-M1 cells (Figure 2C). By contrast, Rlc1p and Cdc15p were not detected in cortical nodes in early mitotic *rng2*-M1 cells (Figures 2B and 2C, arrowheads), although they were detected in cortical nodes or rings in wild-type cells (Figure 2C, asterisk). The localization of myosin II heavy chain, Myo2p, mirrored that of the light chains (Figure S2C). Cdc4p (Figure 2D) and Rlc1p (Figure S2D) failed to localize to cortical nodes in *rng2* null mutants, and the localization of Cdc12p was severely affected in *rng2* null mutants (Figure S2E), establishing that the defective localization of ring components in *rng2*-M1 is not an allele-specific effect. Mid1p localization to cortical nodes was not affected in *rng2* null mutants (Figure S2F). In addition, localization of Rlc1p, Rng2p, and Cdc12p, but not Mid1p, to cortical nodes was severely affected in *cdc4Δ* cells (Rng2p in Figure 2E; Rlc1p, Cdc12p, and Mid1p in Figures S2D–S2F).

Rng2p and Cdc4p were detected in cortical nodes or misorganized rings in early mitotic cells lacking Myo2p (Figure 2F; Rng2p localized in 46 out of 50 cells and Cdc4p localized in 35 out of 35 cells), further establishing that Myo2p functions downstream of Rng2p and Cdc4p.

The fact that Cdc4p localized to cortical nodes in *cdc15Δ*, *cdc12-112* (data not shown), and *myo2Δ* cells and that Rng2p localized to nodes in *myo2Δ* cells (Figure 2F) ruled out the possibility that the loss of any of the node components might destabilize the entire node. We concluded that Rng2p and its binding partner Cdc4p functioned downstream of Mid1p and played a specific role in recruiting myosin II, Cdc15p, and a significant proportion of Cdc12p to cortical nodes. Because Cdc4p failed to localize to nodes in 20 out of 20 *rng2Δ* cells with ≥2 short spindles (Figure 2D) and because Rng2p failed to localize to nodes in 20 out of 20 *cdc4Δ* cells with ≥2 short spindles (Figure 2E), we concluded that Cdc4p and Rng2p display a mutual dependence to localize to the cortical nodes. We note that although assembly

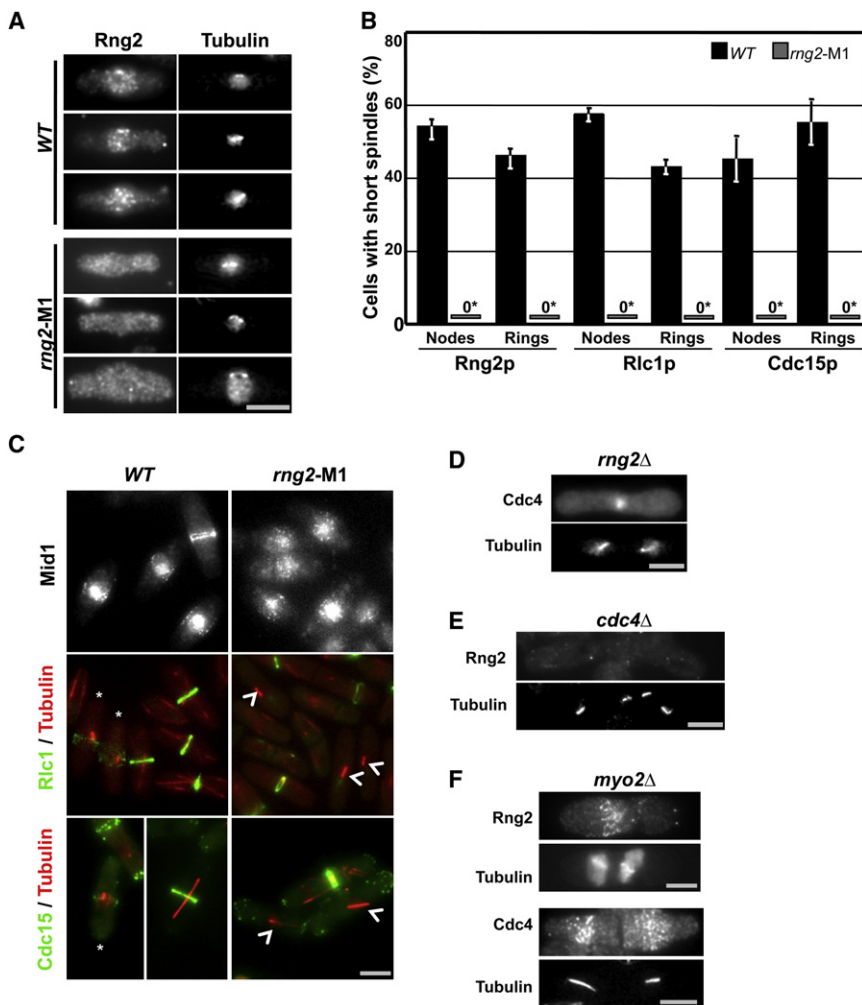


Figure 2. Rng2p Functions Downstream of Mid1p but Upstream of Myosin II and Cdc15p in Cortical Node Organization and Ring Positioning (A) Wild-type Rng2p localizes to cortical nodes during early mitosis, but Rng2-M1p does not. WT (*rng2⁺*) and *rng2*-M1 cells expressing Rng2p-GFP and Rng2-M1p-GFP fusion, respectively, were grown at 24°C, fixed, and stained with GFP and tubulin antibodies.

(B) Quantification of early mitotic WT (n = 50) and *rng2*-M1 (n = 25) cells containing Rng2p, Rlc1p, and Cdc15p in cortical nodes or fully formed actomyosin rings. Mean ± SD (error bars) was plotted based on three independent counts.

(C) Mid1p is detected in cortical nodes in *rng2*-M1 cells, but Rlc1p and Cdc15p are not. WT and *rng2*-M1 cells expressing Mid1p-GFP, Rlc1p-3GFP mCherry-Atb2p, or Cdc15p-GFP mCherry-Atb2p were grown and imaged at 24°C. Mid1p-GFP formed medial nodes in WT and *rng2*-M1 cells, whereas Rlc1p-3GFP and Cdc15p-GFP nodes were observed during early mitosis in WT, but not in *rng2*-M1 cells. Arrowheads indicate *rng2*-M1 cells in early mitosis, and asterisks identify WT cells in early mitosis. Maximum-intensity projections of Z stacks of 0.25 μm are shown.

(D and E) Interdependency of Rng2p and Cdc4p for their localization to the medial nodes. *cdc4Δ* spores expressing Rng2p-GFP and *rng2Δ* spores were germinated at 24°C for 18–22 hr, fixed, and stained with antibodies against GFP and Cdc4p, respectively. In both cases, germinated spores were stained with tubulin antibodies. Cdc4p was not detected in cortical nodes in 20 out of 20 germinated *rng2Δ* spores with two or more short spindles. Similarly, Rng2p was not detected in cortical nodes in 20 out of 20 germinated *cdc4Δ* spores.

(F) Rng2p and Cdc4p localize to cortical nodes in the absence of Myo2p. Rng2p-GFP expressing *myo2Δ* spores were germinated at 24°C for 18–22 hr, fixed, and stained with GFP and tubulin antibodies. In addition, *myo2Δ* spores were germinated at 24°C for 18–22 hr, fixed, and stained with Cdc4p and tubulin antibodies (scale bar represents 5 μm). See also Figure S2.

of myosin II and Cdc15p was completely abolished, Cdc12p assembled into cortical nodes in 15%–20% of *rng2Δ* and *cdc4Δ* cells (Figure S2E). This suggests that a minor Rng2p-independent pathway might contribute toward the organization of Cdc12p nodes.

Next we investigated the mechanism of actomyosin ring mispositioning in *rng2*-M1. The dynamics of Mid1p (upstream of Rng2p) and Rlc1p (downstream of Rng2p) were assessed. We first investigated the behavior of Mid1p in wild-type and *rng2*-M1 by imaging cells expressing Mid1p-GFP and mCherry-Atb2p at 24°C. In wild-type cells, Mid1p was detected in the nucleus and the overlying cortex in interphase, released from the nucleus upon entry into mitosis [3], and incorporated into the actomyosin ring early in mitosis (Figure 3A; time point 10 min; Mid1p incorporated into rings in 16 out of 16 cells imaged). As in wild-type, in *rng2*-M1, Mid1p-GFP was detected in the nucleus and the overlying cortex in interphase and released from the nucleus early in mitosis (Figure 3B). However, unlike in wild-type, Mid1p failed to organize into a ring structure even at later stages of mitosis and trailed away toward the cell ends (Figure 3B; trailing aggregates [nodes] marked with arrowheads). Mid1p was

not detected in compacted rings in 13 out of 16 cells imaged and was detected in faintly compacted rings in the other three cells. Prior to anaphase, the Mid1p cortical band was approximately 3 μm in both wild-type and *rng2*-M1 (Figure S3). Whereas the width of the Mid1p band decreased concomitantly with ring assembly in wild-type, the width of the Mid1p-GFP band increased to approximately 4.5 μm in *rng2*-M1 (Figure S3). These studies establish that defects in Rng2p function lead to the dispersal of Mid1p away from the medial cortex.

To better characterize the behavior of Mid1p with respect to actomyosin rings, we imaged wild-type and *rng2*-M1 cells expressing Mid1p-GFP and Rlc1p-mCherry at 24°C. In 38 out of 38 wild-type cells, the actomyosin ring was formed roughly at the center of the cortical band of Mid1p (Figure 3C; final frame shows a stack of all the time points). However, in a majority of *rng2*-M1 cells (51 out of 77), the actomyosin ring was not formed at the center of the cortical Mid1p band even at the permissive temperature of 24°C (Figure 3D; final frame shows a stack of all the time points), illustrating that the actomyosin ring in *rng2*-M1 cells is assembled outside of the region occupied by Mid1p.

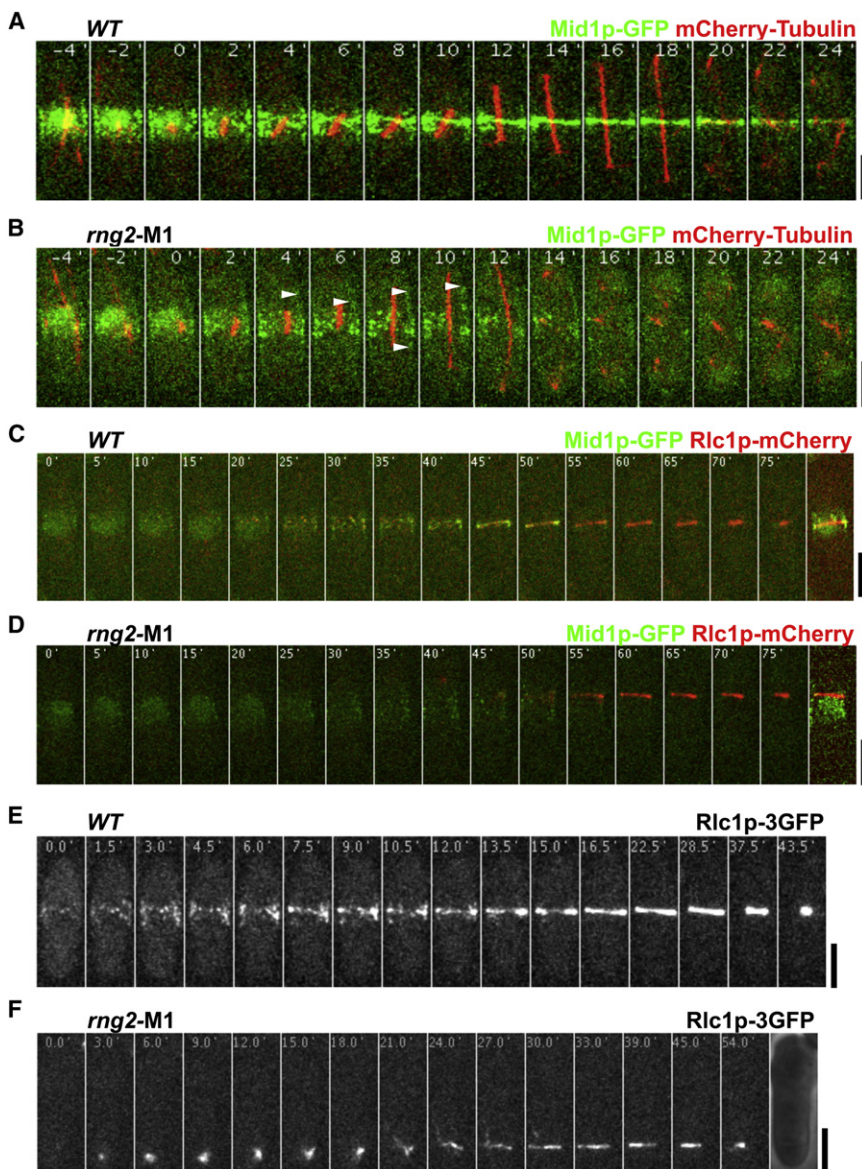


Figure 3. Dynamics of Mid1p and Rlc1p in *rng2-M1*

(A and B) Mid1p fails to incorporate into rings and drifts away from the medial cortex in *rng2-M1* cells. WT and *rng2-M1* cells expressing Mid1p-GFP and mCherry-Atb2p were grown and imaged at 24°C. The time of assembly of a short spindle in cells lacking interphase microtubules was taken as time 0. Arrowheads indicate Mid1p nodes trailing off the medial cortex in *rng2-M1* cells. Images shown are maximum-intensity Z projections of 0.5 μm thick planes.

(C and D) Actomyosin rings do not assemble in the center of the region occupied by the Mid1p cortical band. WT and *rng2-M1* cells expressing Mid1p-GFP and Rlc1p-mCherry were grown and imaged at 24°C. To analyze the position of ring assembly relative to Mid1p localization, we superimposed the time-lapse images in every panel onto a single plane, as shown by the last image in each panel.

(E and F) Rlc1p rings originate from cortical nodes in wild-type but from a single and often off-centered location in *rng2-M1* cells. WT and *rng2-M1* cells expressing Rlc1p-3GFP were grown at 24°C, shifted to 30°C for 3 hr, and imaged at 30°C. Maximum-intensity projections of Z stacks of 0.25 μm are shown. Scale bar represents 5 μm. See also Figure S3.

of these two proteins. To this end, we transformed cells expressing a PK-tagged Rng2p with plasmids weakly overproducing GFP or GFP-Mid1p. Upon immunoblotting, Rng2p-PK was clearly detected as a 160 kDa band (blue asterisks in Figure 4A). Similarly, antibodies against GFP detected GFP and GFP-Mid1p (green asterisks in Figure 4A) in cells expressing these fusions. Immune complexes were generated from *rng2-PK* cells expressing GFP or GFP-Mid1p using antibodies either against GFP or against PK. Antibodies against PK precipitated GFP-Mid1p in cells expressing GFP-Mid1p, but not in cells expressing GFP alone.

In the converse experiment, antibodies against GFP precipitated Rng2p-PK in cells expressing GFP-Mid1p, but not in cells expressing GFP alone. We concluded that Mid1p physically associates with Rng2p, although this interaction might be weak and hence undetectable in wild-type cells.

Given the physical interaction between Mid1p and Rng2p, we investigated whether Mid1p levels were affected in *rng2-M1* cells. Compared to wild-type cells, the level of Mid1p was significantly reduced in *rng2-M1* (Figure 4B). The levels of the soluble and the total fraction of Mid1p were similarly affected (Figure 4B). However, the levels of tubulin (loading control) and other ring proteins tested (actin, Cdc3p, Cdc4p, Cdc8p) were similar in wild-type and *rng2-M1* (Figure 4C). We concluded that *rng2-M1* caused a dramatic reduction in the cellular levels of Mid1p, but not in other actin cytoskeletal components tested.

The ability of Rng2p to bind as well as stabilize Mid1p suggested two possibilities: (1) the actomyosin ring-positioning defect in *rng2-M1* might simply result from destabilization of

The fact that Mid1p drifted away from the cell middle and did not incorporate into actomyosin rings suggested two possible mechanisms for ring misplacement in *rng2-M1*: (1) actomyosin ring assembly might initiate in the medial region of the cell but might drift away from the center or (2) ring assembly might initiate from random locations. To distinguish between these possibilities, we imaged Rlc1p-3GFP in wild-type and *rng2-M1* cells. Rlc1p ring assembly in 33 out of 33 wild-type cells initiated from a series of cortical nodes (Figure 3E). However, in a majority of *rng2-M1* cells (26 out of 32), as in *mid1* mutants, actomyosin rings assembled from a “spot” placed off center (Figure 3F) [5, 7]. These experiments established that actomyosin ring assembly in *rng2-M1* cells is initiated at nonmedial locations in a node-independent manner.

Although phenotypic analysis suggested a physical interaction between Mid1p and Rng2p, we were unable to detect such an interaction when the two proteins were expressed at native levels. We then tested whether a physical interaction between Mid1p and Rng2p is detected upon increase in the level of one

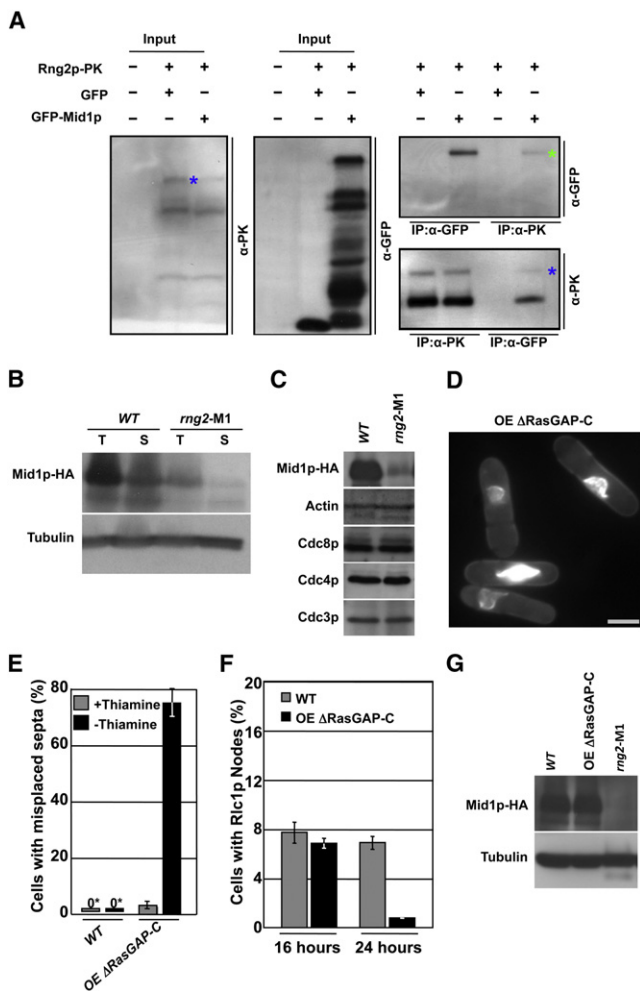


Figure 4. Rng2p Physically Interacts with Mid1p

(A) Weakly overexpressed Rng2p physically interacts with Mid1p. Lysates were prepared from cells expressing PK-tagged Rng2p and simultaneously overexpressing either GFP or GFP-Mid1p (from the weak *nmt1* promoter). Immune complexes were generated using antibodies against PK or GFP, separated by electrophoresis, and immunoblotted with antibodies against PK or GFP.

(B) Mid1p levels are reduced in *rng2-M1* cells. Total (T) and soluble (S) proteins were extracted from WT and *rng2-M1* cells expressing Mid1p-3HA and immunoblotted with antibodies against HA or tubulin.

(C) The levels of Cdc3p, Cdc4p, Cdc8p, and Act1p are not altered in *rng2-M1* cells. Total cell lysates were prepared from WT and *rng2-M1* cells and immunoblotted with antibodies against Cdc3p, Cdc4p, Cdc8p, Act1p, and HA.

(D) Overexpression of Rng2p lacking RasGAP-C results in misplaced septa. Wild-type cells overexpressing GFP-Rng2p Δ RasGAP-C were fixed and stained with aniline blue.

(E) Quantification of septum positioning in WT cells and in cells overexpressing Rng2p lacking the RasGAP-C domain (OE Rng2p Δ RasGAP-C). Mean \pm SD (error bars) was based on three independent experiments (n = 500).

(F) Overproduction of Rng2p Δ RasGAP-C leads to defects in Rlc1p-mCherry cortical node organization. WT cells expressing Rlc1p-mCherry and carrying an empty plasmid (WT) or a plasmid overexpressing GFP-Rng2p Δ RasGAP-C (OE Δ RasGAP-C) were grown under conditions that induce expression from the *nmt1* promoter. Samples were taken at 16 hr and 24 hr after induction, and the number of unseptated cells with cortical nodes of Rlc1p-mCherry was estimated. Over 1000 cells were scored in each case. The data shown is the mean \pm SD (error bars) of two independent experiments.

(G) The stability of Mid1p is not affected upon overexpression of GFP-Rng2p Δ RasGAP-C. Total cell lysates were prepared from wild-type and

Mid1p or, alternatively, (2) it is possible that Rng2p both plays a role in recruiting actomyosin ring components to cortical nodes and functions independently in Mid1p stabilization. Mid1p is clearly detected by fluorescence microscopy in *rng2-M1* and *rng2* null mutants. However, Cdc4p, Rlc1p, Cdc12p, and Cdc15p are not detected in even fainter node-like structures in *rng2-M1* and *rng2* null mutants, suggesting that Mid1p-bound Rng2p directly plays a role in recruiting actomyosin ring components to cortical nodes.

This view was reinforced by an independent set of experiments aimed at understanding Rng2p structure-function relationships, wherein overproduction of Rng2p lacking RasGAP-C (known to localize to rings but not to nodes [9]) generated a strong defect in septum positioning (Figures 4D and 4E). Overproduction of Rng2p lacking RasGAP-C also led to a dramatic reduction in the number of cells with Rlc1p-mCherry nodes (Figure 4F). We then compared the levels of Mid1p in wild-type cells, *rng2-M1* cells, and cells overproducing Rng2p Δ RasGAP-C. The level of Mid1p in cells overproducing Rng2p Δ RasGAP-C, but not in *rng2-M1* cells, was similar to that in wild-type cells (Figure 4G). We conclude that alteration of Rng2p function, notwithstanding the presence of normal levels of Mid1p, can lead to defects in cortical node organization and actomyosin ring positioning.

In summary, we have shown that Rng2p and its binding partner Cdc4p function downstream of Mid1p to organize actomyosin ring components such as Cdc12p, Cdc15p, and myosin II into cortical nodes (see graphical abstract available online). Different domains of Rng2p might promote physical interaction with different interacting partners. It is likely that RasGAP-C participates in binding Mid1p, because the localization of Rng2p to cortical nodes, but not the actomyosin ring, is abolished in *rng2-M1*, as well as in cells expressing Rng2p Δ RasGAP-C [9]. Other sequences, such as the CHD and the IQ motifs, might participate in interactions with actomyosin ring components such as Cdc4p, F-actin, and Cdc15p [9, 17, 22]. Because Rng2p also plays a role in Mid1p stability, it is possible that Rng2p binding, followed by compaction of Mid1p nodes into a ring, stabilizes Mid1p at the division site.

Supplemental Information

Supplemental Information includes Supplemental Experimental Procedures, three figures, and one table and can be found with this article online at doi:10.1016/j.cub.2011.01.059.

Acknowledgments

We would like to acknowledge Kathy Gould, Keith Gull, Kentaro Nakano, Tom Pollard, Masamitsu Sato, and Jian-Qiu Wu for research material. Special thanks are due to Jian-Qiu Wu for discussion of related research work from his group. We would like to thank all members of the Balasubramanian laboratory and Snezhana Olfiferenko for discussion, as well as Yinyi Huang, Meredith Calvert, Ramanujam Srinivasan, and Dhivya Subramaniam for critical reading of the manuscript and Xu Liang for technical help. This work was supported by research funds from the Singapore Millennium Foundation.

Received: August 26, 2010

Revised: December 22, 2010

Accepted: January 24, 2011

Published online: March 3, 2011

rng2-M1 expressing Mid1p-3HA, as well as from cells overexpressing GFP-Rng2p Δ RasGAP-C (OE Δ RasGAP-C) and coexpressing normal levels of Mid1p-3HA, and immunoblotted using antibodies against the HA-epitope and tubulin. Scale bar represents 5 μ m.

References

1. Sohrmann, M., Fankhauser, C., Brodbeck, C., and Simanis, V. (1996). The *dmf1/mid1* gene is essential for correct positioning of the division septum in fission yeast. *Genes Dev.* 10, 2707–2719.
2. Bähler, J., Steever, A.B., Wheatley, S., Wang, Y., Pringle, J.R., Gould, K.L., and McCollum, D. (1998). Role of polo kinase and Mid1p in determining the site of cell division in fission yeast. *J. Cell Biol.* 143, 1603–1616.
3. Paoletti, A., and Chang, F. (2000). Analysis of *mid1p*, a protein required for placement of the cell division site, reveals a link between the nucleus and the cell surface in fission yeast. *Mol. Biol. Cell* 11, 2757–2773.
4. Wu, J.Q., Kuhn, J.R., Kovar, D.R., and Pollard, T.D. (2003). Spatial and temporal pathway for assembly and constriction of the contractile ring in fission yeast cytokinesis. *Dev. Cell* 5, 723–734.
5. Motegi, F., Mishra, M., Balasubramanian, M.K., and Mabuchi, I. (2004). Myosin-II reorganization during mitosis is controlled temporally by its dephosphorylation and spatially by Mid1 in fission yeast. *J. Cell Biol.* 165, 685–695.
6. Wu, J.Q., Sirotkin, V., Kovar, D.R., Lord, M., Beltzner, C.C., Kuhn, J.R., and Pollard, T.D. (2006). Assembly of the cytokinetic contractile ring from a broad band of nodes in fission yeast. *J. Cell Biol.* 174, 391–402.
7. Huang, Y., Yan, H., and Balasubramanian, M.K. (2008). Assembly of normal actomyosin rings in the absence of Mid1p and cortical nodes in fission yeast. *J. Cell Biol.* 183, 979–988.
8. Eng, K., Naqvi, N.I., Wong, K.C., and Balasubramanian, M.K. (1998). Rng2p, a protein required for cytokinesis in fission yeast, is a component of the actomyosin ring and the spindle pole body. *Curr. Biol.* 8, 611–621.
9. Takaine, M., Numata, O., and Nakano, K. (2009). Fission yeast IQGAP arranges actin filaments into the cytokinetic contractile ring. *EMBO J.* 28, 3117–3131.
10. Kuroda, S., Fukata, M., Kobayashi, K., Nakafuku, M., Nomura, N., Iwamatsu, A., and Kaibuchi, K. (1996). Identification of IQGAP as a putative target for the small GTPases, Cdc42 and Rac1. *J. Biol. Chem.* 271, 23363–23367.
11. Adachi, H., Takahashi, Y., Hasebe, T., Shirouzu, M., Yokoyama, S., and Sutoh, K. (1997). Dictyostelium IQGAP-related protein specifically involved in the completion of cytokinesis. *J. Cell Biol.* 137, 891–898.
12. Erickson, J.W., Cerione, R.A., and Hart, M.J. (1997). Identification of an actin cytoskeletal complex that includes IQGAP and the Cdc42 GTPase. *J. Biol. Chem.* 272, 24443–24447.
13. Tang, X., Huang, J., Padmanabhan, A., Bakka, K., Bao, Y., Yuelin Tan, B., Zacheus Cande, W., and Balasubramanian, M.K. (2010). Marker reconstitution mutagenesis: A simple and efficient reverse genetic approach. *Yeast.* 10.1002/yea.1831.
14. Chang, F., Woollard, A., and Nurse, P. (1996). Isolation and characterization of fission yeast mutants defective in the assembly and placement of the contractile actin ring. *J. Cell Sci.* 109, 131–142.
15. Balasubramanian, M.K., McCollum, D., Chang, L., Wong, K.C., Naqvi, N.I., He, X., Sazer, S., and Gould, K.L. (1998). Isolation and characterization of new fission yeast cytokinesis mutants. *Genetics* 149, 1265–1275.
16. Naqvi, N.I., Eng, K., Gould, K.L., and Balasubramanian, M.K. (1999). Evidence for F-actin-dependent and -independent mechanisms involved in assembly and stability of the medial actomyosin ring in fission yeast. *EMBO J.* 18, 854–862.
17. D'souza, V.M., Naqvi, N.I., Wang, H., and Balasubramanian, M.K. (2001). Interactions of Cdc4p, a myosin light chain, with IQ-domain containing proteins in *Schizosaccharomyces pombe*. *Cell Struct. Funct.* 26, 555–565.
18. Cerutti, L., and Simanis, V. (1999). Asymmetry of the spindle pole bodies and *spg1p* GAP segregation during mitosis in fission yeast. *J. Cell Sci.* 112, 2313–2321.
19. Wolfe, B.A., and Gould, K.L. (2005). Split decisions: Coordinating cytokinesis in yeast. *Trends Cell Biol.* 15, 10–18.
20. Krapp, A., Gulli, M.P., and Simanis, V. (2004). SIN and the art of splitting the fission yeast cell. *Curr. Biol.* 14, R722–R730.
21. Hachet, O., and Simanis, V. (2008). Mid1p/anillin and the septation initiation network orchestrate contractile ring assembly for cytokinesis. *Genes Dev.* 22, 3205–3216.
22. Roberts-Galbraith, R.H., Ohi, M.D., Ballif, B.A., Chen, J.S., McLeod, I., McDonald, W.H., Gygi, S.P., Yates, J.R., 3rd, and Gould, K.L. (2010). Dephosphorylation of F-BAR protein Cdc15 modulates its conformation and stimulates its scaffolding activity at the cell division site. *Mol. Cell* 39, 86–99.